Astronomy & Astrophysics manuscript no. 13700
December 16, 2009

Absolute dimensions of eclipsing binaries. ⋆

XXVII. V1130 Tauri: A metal-weak F-type system, perhaps with preference for $Y = 0.23 - 0.24$ ⋆⋆

J.V. Clausen[1], E.H. Olsen[1], B.E. Helt[1], and A. Claret[2]

[1] Niels Bohr Institute, Copenhagen University, Juliane Maries Vej 30, DK-2100 Copenhagen Ø, Denmark
[2] Instituto de Astrofísica de Andalucía, CSIC, Apartado 3004, E-18080 Granada, Spain

Received 20 November 2009 / Accepted 4 December 2009

ABSTRACT

Context. Double-lined, detached eclipsing binaries are our main source for accurate stellar masses and radii. This paper is the first in a series with focus on the upper half of the main-sequence band and tests of 1–2 $M_\odot$ evolutionary models.
Aims. We aim to determine absolute dimensions and abundances for the detached eclipsing binary V1130 Tau, and to perform a detailed comparison with results from recent stellar evolutionary models.
Methods. *uvby* light curves and *uvbyβ* standard photometry have been obtained with the Strömgren Automatic Telescope, and high-resolution spectra have been acquired at the FEROS spectrograph; both are ESO, La Silla facilities. We have applied the Wilson-Devinney model for the photometric analysis, spectroscopic elements are based on radial velocities measured via broadening functions, and [Fe/H] abundances have been determined from synthetic spectra and *uvby* calibrations.
Results. V1130 Tau is a bright ($m_V = 6.56$), nearby (71 ± 2 pc) detached system with a circular orbit ($P = 0\overset{\mathrm{d}}{.}80$). The components are deformed with filling factors above 0.9. Their masses and radii have been established to 0.6–0.7%. We derive a [Fe/H] abundance of -0.25 ± 0.10. The measured rotational velocities, 92.4 ± 1.1 (primary) and 104.7 ± 2.7 (secondary) km s^{-1}, are in fair agreement with synchronization. The larger 1.39 $M_\odot$ secondary component has evolved to the middle of the main-sequence band and is slightly cooler than the 1.31 $M_\odot$ primary. Yonsai-Yale, BaSTI, and Granada evolutionary models for the observed metal abundance and a 'normal' He content of $Y = 0.25-0.26$, marginally reproduce the components at ages between 1.8 and 2.1 Gyr. All such models are, however, systematically about 200 K hotter than observed and predict ages for the more massive component, which are systematically higher than for the less massive component. These trends can not be removed by adjusting the amount of core overshoot or envelope convection level, or by including rotation in the model calculations. They may be due to proximity effects in V1130 Tau, but on the other hand, we find excellent agreement for 2.5–2.8 Gyr Granada models with a slightly lower Y of 0.23–0.24.
Conclusions. V1130 Tau is a valuable addition to the very few well-studied 1–2 $M_\odot$ binaries with component(s) in the upper half of the main-sequence band, or beyond. The stars are not evolved enough to provide new information on the dependence of core overshoot on mass (and abundance), but might - together with a larger sample of well-detached systems - be useful for further tuning of the helium enrichment law. Analyses of such systems are in progress.

Key words. Stars: evolution – Stars: fundamental parameters – Stars: individual: V1130 Tau – Stars: binaries: eclipsing – Techniques: photometric – Techniques: radial velocities

1. Introduction

In this paper, we present the first detailed study of the bright ($m_V = 6.56$), early F-type, double-lined eclipsing binary V1130 Tau. The orbital period is short ($P = 0\overset{\mathrm{d}}{.}80$), but the system is still detached, and for several reasons it is an interesting case. First, it is more evolved than most of the well studied early F-type main sequence systems; actually the more massive, larger component has become the slightly cooler one. Next, it is reported to be metal-weak. Finally, it is situated at a distance of only 71 pc, meaning that it belongs to the (small) group of eclipsing binaries within 125 pc, discussed by Popper (1998), which could be useful for improving the radiative flux scale.

In the following, we determine absolute dimensions and abundances, based on analyses of new *uvby* light curves and high-resolution spectra, and compare V1130 Tau to several modern stellar evolutionary models. Throughout the paper, the component eclipsed at the slightly deeper eclipse at phase 0.0 is referred to as the primary (p), and the other as the secondary (s) component.

2. V1130 Tau

HD 24133 (CSV 356, HIP 17988) was confirmed to be variable by Olsen (1983). Based on the *uvby* photometry, Olsen supplied Abt with a list containing about 800 po-

Send offprint requests to: J.V. Clausen,
e-mail: jvc@nbi.ku.dk

⋆ Based on observations carried out at the Strömgren Automatic Telescope (SAT) and the 1.5m telescope at ESO, La Silla (62.H-0319, 62.L-0284, 63.H-0080, 64.L-0031, 66.D-0178)

⋆⋆ Table 11 is available in electronic form at the CDS via anonymous ftp to cdsarc.u-strasbg.fr (130.79.128.5) or via http://cdsweb.u-strasbg.fr/cgi-bin/qcat?J/A+A/

Table 1. Photometric data for V1130 Tau and the comparison stars.

Object	Sp. Type	Ref.	V	σ	$b-y$	σ	m_1	σ	c_1	σ	N($uvby$)	β	σ	N(β)
V1130 Tau	F2 V[a]	C10	6.556	9	0.263	3	0.140	7	0.478	9	19	2.653	6	32
		F88	6.594	30	0.272	0	0.136	2	0.478	1	2	2.652		1
		O83	6.639	50	0.276	1	0.124	4	0.474	3	4	2.652	7	3
HD23503	F2/3 V[a]	C10	8.262	6	0.261	5	0.174	8	0.509	9	156	2.686	8	22
		O83	8.251	1	0.272	0	0.163	9	0.510	1	2			
		O94	8.264	5	0.266	3	0.167	4	0.497	6	1	2.666	6	1
HD24552	G1 V[a]	C10	7.979	6	0.386	5	0.200	8	0.325	8	107	2.596	8	16
		O83	7.972	6	0.392	3	0.200	1	0.329	3	2			
		O94	7.975	5	0.387	3	0.196	4	0.326	6	1	2.575	6	1
HD25059	G3 V[a]	C10	9.161	5	0.391	4	0.192	8	0.329	9	101	2.591	9	19
		O93			0.399	3	0.164	5	0.359	6	1			
		O94	9.163	4	0.392	3	0.185	5	0.335	7	1	2.583	6	1

[a] Houk & Swift (1999); for V1130 Tau, see also spectral types in Sect. 2

NOTE 1: References are: C10 = This paper, F88 = Franco (1988), O83 = Olsen (1983), O93 = Olsen (1993), O94 = *uvby*: Olsen (1994), β: Olsen (unpublished).
NOTE 2: For V1130 Tau, the *uvby* information by C09 is the mean value at phases 0.25 and 0.75, and the β information is the mean value outside eclipses.
NOTE 3: N is the total number of observations used to form the mean values, and σ is the rms error (per observation) in mmag.

tentially weak-lined A5-G0 stars, and Abt (1986) subsequently classified HD 24133 as F3 V wl (A5 met) and also reported it to be a double-lined spectroscopic binary. Gray (1989) classified HD 24133 as F5 V m-2, Gray & Garrison 1989) confirmed that its metal lines have the strength of an A5 star, and Gray et al. (2001) found it to be a fairly rapid rotator, but clearly metal-weak. The eclipsing nature was discovered by Hipparcos (ESA 1997; orbital period $0\overset{\mathrm{d}}{.}7988710$), and HD 24133 was subsequently assigned the variable name V1130 Tau (Kazarovets et al. 1999). Rucinski et al. (2003) determined a spectroscopic orbit, leading to $(M_p + M_s)\sin^3 i = 2.41 \pm 0.03\ M_\odot$, and noted that V1130 Tau is one of the shortest period detached early F-type systems. Besides a few times of minima, nothing has been published on this binary since then.

3. Photometry

Below, we present the new photometric material for V1130 Tau and refer to Clausen et al. (2001; hereafter CHO01) for further details on observation and reduction procedures, and determination of times of minima.

3.1. Light curves for V1130 Tau

The differential *uvby* light curves of V1130 Tau were observed at the Strömgren Automatic Telescope (SAT) at ESO, La Silla and its 6-channel *uvbyβ* photometer on 59 nights between October 1997 and November 1998 (JD2450727–2451120). They contain 583 points per band with all phases covered at least twice. The observations were done through an 18 arcsec diameter circular diaphragm at airmasses between 1.2 and 1.8. HD 23503, HD 24552, and HD 25059 - all within a few degrees from V1130 Tau on the sky - were used as comparison stars and were all found to be constant within a few mmag; see Table 1. The light curves were calculated relative to HD 23503, but all comparison star observations were used, shifting them first to the same light level. The average accuracy per point is about 4–5 mmag (*ybv*) and 7 mmag (*u*).

As seen from Fig. 1, V1130 Tau is detached but fairly close, with *y* eclipse depths of about 0.4 mag. Primary eclipse is only marginally deeper than secondary, meaning that the surface fluxes of the components are nearly identical. The light curves (Table 11) will only be available in electronic form.

3.2. Standard photometry for V1130 Tau

Standard *uvbyβ* indices for V1130 Tau (between eclipses) and the three comparison stars, observed and derived as described by CHO01, are presented in Table 1. The indices are based on many observations and their precision is high. For comparison, we have included published photometry from other sources. In general, the agreement is good, but individual differences larger than the quoted errors occur.

3.3. Times of minima and ephemeris for V1130 Tau

Three times of each of primary and secondary minimum have been established from the *uvby* light curve observations; see Table 2. A list of earlier times of minima was kindly provided by Kreiner; see Kreiner et al. (2001) and Kreiner (2004)[1]. Except for two unpublished times based on Hipparcos photometry, which showed large deviations, they were included in the ephemeris analysis together with the recently published time of primary minimum by Brat et al. (2008).

Assuming a circular orbit, we derive the following linear ephemeris from a weighted least squares fit to all accepted times of minima:

$$\mathrm{Min\ I} = \begin{array}{l} 2450770.69601 \\ \pm 9 \end{array} + \begin{array}{l} 0\overset{\mathrm{d}}{.}798868143 \\ \pm 38 \end{array} \times E \quad (1)$$

Separate weighted linear least squares fits to the times of primary and secondary minima lead to identical orbital pe-

[1] http://www.as.ap.krakow.pl/ephem

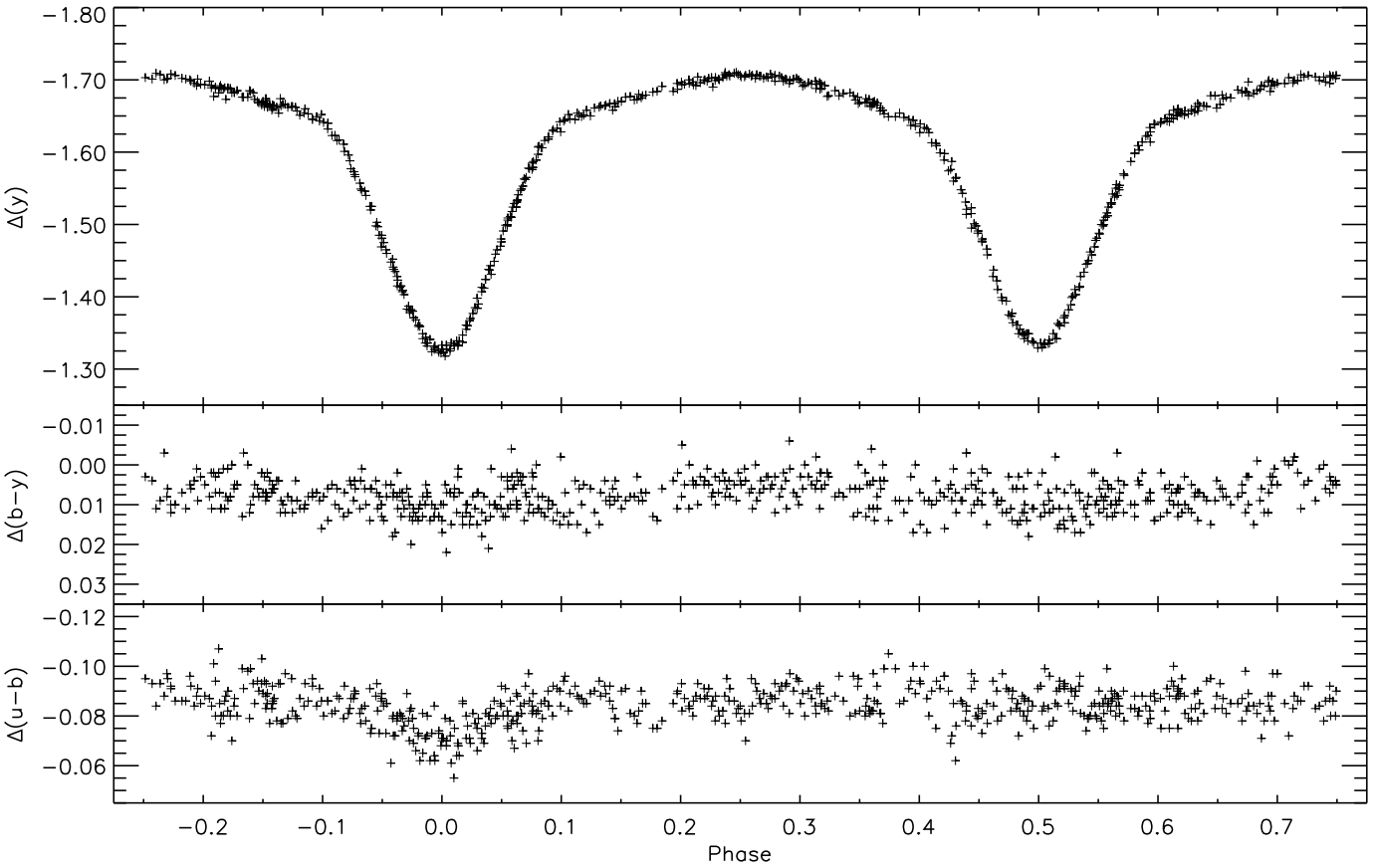

Fig. 1. y light curve and $b-y$ and $u-b$ colour curves (instrumental system) for V1130 Tau.

Table 2. Times of primary (P) and secondary (S) minima of V1130 Tau determined from the *uvby* observations.

HJD − 2 400 000	rms	Type	O-C[a]
50742.73603	0.00040	P	0.00041
50770.69594	0.00020	P	−0.00007
50778.68480	0.00020	P	0.00011
50774.73329	0.00040	S	0.00049
50776.68754	0.00020	S	0.00002
50780.68191	0.00020	S	0.00005

[a] Calculated from the ephemeris given in Eq. 1

riods, and we adopt Eq. 1 for the analyses of the *uvby* light curves and radial velocities.

3.4. Photometric elements

Since the relative radii of the components of V1130 Tau are fairly large, 0.25–0.30, we have adopted the Wilson-Devinney model (Wilson & Devinney 1971; Wilson 1979, 1990, 1993; Van Hamme & Wilson 2003) for the light curve analyses. We have used the JKTWD code developed by J. Southworth[2], which is based on the 2003 version of the 'Binary Star Observables Program' by Wilson et al.[3] This code was recently applied for the light curve analyses of DW Car (Southworth & Clausen 2007) and V380 Cyg (Pavlovski et al. 2009).

Mode 2 (detached binaries) was used throughout, and the stellar atmosphere approximation functions for the *uvby* bands were adopted (Van Hamme & Wilson 2003, Kurucz 1993). The effective temperature of the primary component was kept at 6500 K; see Sect. 6. A linear limb darkening law was assumed with coefficients adopted from Van Hamme (1993). The linear coefficients by Claret (2000) are about 0.1 larger and lead to a 0°.2 lower orbital inclination, whereas the radii are practically unchanged. Within errors, non-linear limb darkening lead to identical photometric elements. Gravity darkening exponents corresponding to convective atmospheres were applied, and bolometric reflection albedo coefficients of 0.5 were chosen, again due to convection. The simple reflection mode (MREF = 1) was used; we note that the detailed mode gives nearly identical elements. The mass ratio between the components was kept at the spectroscopic value ($M_s/M_p = 1.066 \pm 0.004$), and synchronous rotation was assumed. The light curves were analysed independently with at least 10 differential param-

[2] http://www.astro.keele.ac.uk/∼jkt/

[3] ftp://ftp.astro.ufl.edu/pub/wilson/

Table 3. Photometric solutions for V1130 Tau.

	y	b	v	u
i (°)	73.97 ±2	73.84 ±4	73.73 ±4	74.20 ±6
Ω_p	4.5138 ±39	4.5079 ±40	4.4954 ±41	4.5642 ±64
Ω_s	4.0727 ±25	4.0753 ±29	4.0775 ±30	4.0805 ±45
r_p	0.2956	0.2961	0.2973	0.2911
r_s	0.3542	0.3539	0.3536	0.3532
k	1.198	1.195	1.189	1.213
$r_p + r_s$	0.6498	0.6500	0.6509	0.6443
$u_p = u_s$	0.52	0.61	0.67	0.63
$T_{\rm eff,s}$	6638 ±4	6639 ±3	6643 ±3	6628 ±4
L_s/L_p	1.444	1.436	1.429	1.436
σ (mmag.)	4.5	4.3	4.3	6.5

NOTE 1: Limb darkening coefficients by van Hamme (1993), gravity darkening exponents of 0.33, and bolometric albedo coefficients of 0.5 were adopted, as appropriate for convective envelopes. $T_{\rm eff,p}$ was assumed to be 6650 K, see Sect. 6.
NOTE 2: The errors quoted for the free parameters are the *formal* standard errors determined from the iterative least squares solution procedure.

Table 4. Adopted photometric elements for V1130 Tau.

i	$73\overset{\circ}{.}82 \pm 0\overset{\circ}{.}20$
r_p	0.2952 ± 0.0018
$r_p(pole)$	0.2862
$r_p(point)$	0.3125
$r_p(side)$	0.2935
$r_p(back)$	0.3048
r_s	0.3535 ± 0.0021
$r_s(pole)$	0.3369
$r_s(point)$	0.3965
$r_s(side)$	0.3506
$r_s(back)$	0.3717

	y	b	v	u
L_s/L_p	1.443 ±23	1.437 ±23	1.432 ±23	1.434 ±23

NOTE: The individual luminosity ratios are based on the mean stellar and orbital parameters.

eter corrections, and continuing until they were below 20% of the corresponding formal standard errors for all parameters. The stability of the adopted solutions was tested by adding 100 more iterations.

In tables and text, we use the following symbols: i orbital inclination; r relative volume radius; $k = r_s/r_p$; Ω surface potential; u linear limb darkening coefficient; L luminosity; $T_{\rm eff}$ effective temperature.

The individual solutions are presented in Table 3, and $O-C$ residuals of the b observations from the theoretical light curve are shown in Fig. 2. Equally good fits are obtained in the three other bands, and the rms of the residuals correspond closely to the observational accuracy. As expected, the less massive, slightly hotter primary component is also the smaller one. V1130 Tau is detached, but the filling factors of the components are above 0.9, and the deformation of the secondary component is significant. The relative volume radii obtained from the four bands agree

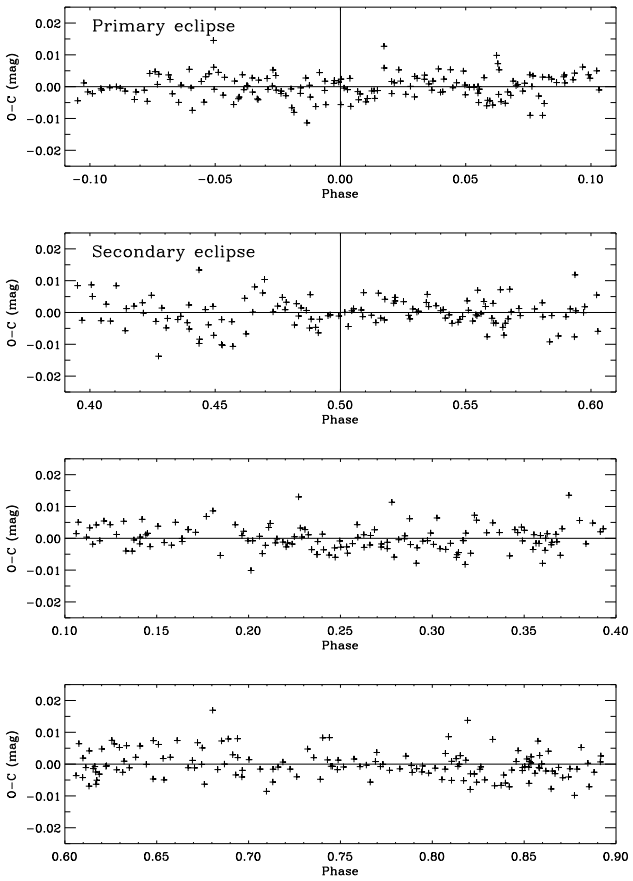

Fig. 2. $(O-C)$ residuals of the V1130 Tau b-band observations from the theoretical light curve computed for the photometric elements given in Table 3.

well, except perhaps for the less precise u result for the primary. We find no evidence of third light, neither in the spectra nor from the light curve solutions, and the small differences in orbital inclinations are probably due to model and/or limb darkening effects. The adopted photometric elements are listed in Table 4 with realistic uncertainties, which reflect the formal standard errors and the interagreement of the *uvby* results, and also take into account the consequences of ±0.1 changes of limb darkening coefficients and the uncertainly of the mass ratio. As seen, the relative volume radii have been established to about 0.6%.

4. Spectroscopy

4.1. Spectroscopic observations

For radial velocity and abundance determinations, we have obtained 18 high-resolution spectra with the FEROS fiber echelle spectrograph at the ESO 1.52-m telescope at La Silla, Chile (Kaufer et al. 1999, 2000). The spectrograph, which resides in a temperature-controlled room, covers without interruption the spectral region from the Balmer jump to 8700 Å, at a constant velocity resolution of 2.7 $\rm km\,s^{-1}$ per pixel ($\lambda/\Delta\lambda = 48\,000$). We refer to Clausen et al. (2008, hereafter CTB08) for details on the reduction of the spectra, which were observed between January 1999 and March 2001; an observing log is given in Table 5.

Table 5. Log of the FEROS observations of V1130 Tau.

HJD−2 400 000[a]	phase	t_{exp}[b]	S/N[c]
51188.6379	0.1675	600	223
51207.5446	0.8344	600	171
51207.5662	0.8615	600	170
51208.5852	0.1370	600	162
51209.5918	0.3971	600	200
51211.5630	0.8645	600	84
51212.6064	0.1706	600	176
51385.9274	0.1288	600	142
51386.9327	0.3872	600	170
51390.8696	0.3154	600	241
51391.9171	0.6266	600	225
51392.8746	0.8252	720	237
51562.5335	0.1992	600	243
51562.5962	0.2777	600	281
51562.6289	0.3187	600	244
51977.4958	0.6371	630	181
51978.4897	0.8812	600	179
51981.4927	0.6402	600	166

[a] Refers to mid-exposure
[b] Exposure time in seconds
[c] Signal-to-noise ratio measured around 6070 Å. At the shorter wavelengths used for the radial velocity measurements it is somewhat lower

Table 6. Echelle orders and wavelength ranges used for the radial velocity measurements of V1130 Tau.

Order	Range (Å)	Order	Range (Å)
55	4020 - 4090	53	4170 - 4240
52	4220 - 4330	50	4395 - 4500
49	4510 - 4590	45	4905 - 4975
44	4975 - 5090	43	5090 - 5212

4.2. Radial velocities

The radial velocities for V1130 Tau were measured from eight useful orders (4020 – 5210 Å) of the 18 FEROS spectra, see Table 6. The selection of this limited number of orders was based on initial analyses, which showed that several orders give unreliable results and have to be excluded, either because too few lines are available, or because they contain defects or are difficult to normalise properly. We applied the broadening function (BF) formalism (Rucinski 1999, 2002, 2004), using synthetic templates with no rotational broadening, calculated for $T_{\rm eff}$ = 6650 K, log(g) = 4.0, and [Fe/H] = −0.25. They were produced with the *bssynth* tool (Bruntt, private communication), which applies the SYNTH software (Valenti & Piskunov 1996) and modified ATLAS9 models (Heiter 2002). Line information was taken from the Vienna Atomic Line Database (VALD; Kupka et al. 1999). BF's were then produced for each of the selected orders of each spectrum.

Due to the deformation of the components (Table 4) and to reflection effects, the lineprofiles and thereby the BF's can not a priori be expected to be symmetric. The optimum method for radial velocity determinations is therefore to fit theoretical BF's which take the proximity effects into account; for W UMa systems, see e.g. Rucinski et al (1993) and references therein. Such BF's were constructed, for both components at each phase and order, from synthetic rotational broadened line profiles calculated via the Wilson-Devinney (WD) model (Sect. 3.4). The radial velocities were then determined by fitting combined theoretical BF's to the observed ones, i.e. by shifting and scaling the theoretical BF's for each component until the best fit was obtained for the combination.

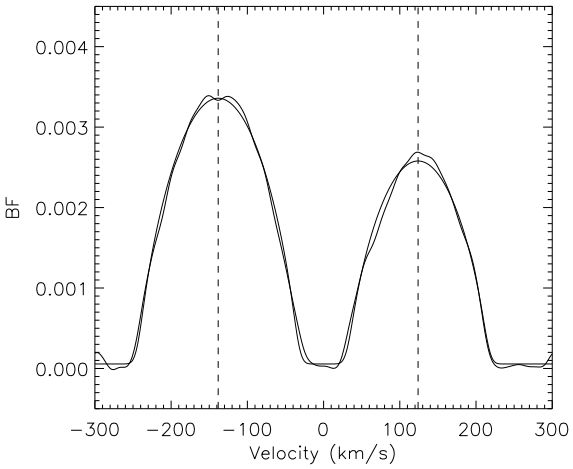

Fig. 3. Broadening function (thick) obtained for the 5090-5212 Å region and theoretical fit (thin). The FEROS spectrum was taken at phase 0.834, at HJD=2451207.5446. The primary component is to the right.

Since the observed BF's do not show clear asymmetries, we have also applied an approach based on simpler theoretical BF's, which assume that the stars are spherical, rigid rotators (e.g. Kaluzny et al. 2006). Before the radial velocity determination, these BF's were convolved with a Gauss profile corresponding to the instrumental resolution. In general, very good fits were obtained from this approach; see Fig. 3.

In the case of V1130 Tau, the two BF approaches result in radial velocities for all spectral orders and phases, which agree within about 1–2 km s^{-1}, and the differences do not correlate with orbital phase and/or velocity separation. In Sect. 4.3 we present orbital solutions from both sets of radial velocities.

As described by e.g. Kaluzny et al. (2006), the projected rotational velocities $v \sin i$ of the components and (monochromatic) light/luminosity ratios between them can also be obtained from analyses of the simple broadening functions mentioned above. We have tested this on synthetic binary spectra with input rotational velocities of 90.0 (primary) and 110.0 (secondary) km s^{-1}, corresponding closely to pseudosynchronous rotation, and a light ratio of 1.44, and we find that the method is safe for V1130 Tau. The rotational velocities determined from the BF analyses are within 1 km s^{-1}from the input values, and the light ratio is reproduced to high precision. Analyses of the observed V1130 Tau spectra yield mean $v \sin i$ velocities of 92.4 ± 1.1 (primary) and 104.7 ± 2.7 km s^{-1}(secondary), and the mean light ratio, 1.44 ± 0.02, is in perfect agreement with the results from the light curve analyses (Table 4). No significant wavelength/order dependencies are seen.

Table 7. Spectroscopic orbital solution for V1130 Tau.

Parameter	WD based BF	Symmetrical BF	Mean velocities Adopted
Adjusted quantities:			
K_p ($\mathrm{km\,s^{-1}}$)	158.14 ± 0.34	158.33 ± 0.37	158.29 ± 0.34
K_s ($\mathrm{km\,s^{-1}}$)	148.45 ± 0.42	148.49 ± 0.27	148.52 ± 0.33
γ_p ($\mathrm{km\,s^{-1}}$)	-10.98 ± 0.27	-11.12 ± 0.30	-11.05 ± 0.28
γ_s ($\mathrm{km\,s^{-1}}$)	-11.03 ± 0.34	-11.41 ± 0.22	-11.22 ± 0.27
Adopted quantities:			
P (days)	0.798868143	0.798868143	0.798868143
T (HJD$-2\,400\,000$)[a]	50770.69601	50770.69601	50770.69601
e	0.00	0.00	0.00
Derived quantities:			
$M_p \sin^3 i$ ($\mathrm{M_\odot}$)	1.155 ± 0.007	1.157 ± 0.005	1.157 ± 0.006
$M_s \sin^3 i$ ($\mathrm{M_\odot}$)	1.230 ± 0.006	1.234 ± 0.006	1.233 ± 0.006
$a \sin i$ ($\mathrm{R_\odot}$)	4.839 ± 0.009	4.843 ± 0.007	4.842 ± 0.007
Other quantities pertaining to the fit:			
N_{obs}	18	18	18
Time span (days)	793	793	793
σ_p ($\mathrm{km\,s^{-1}}$)	1.15	1.26	1.17
σ_s ($\mathrm{km\,s^{-1}}$)	1.42	0.93	1.14

[a] Time of central primary eclipse

4.3. Spectroscopic elements

Spectroscopic orbits have been derived through analyses of the radial velocities obtained from each of the two BF analyses of the eight selected orders. Since the components of V1130 Tau are quite close and deformed, the observed light center velocities deviate somewhat from the center of mass velocities, which are used to determine the Keplerian orbital parameters. Before analysing the velocities, we have therefore for each order applied phase dependent corrections as calculated from the Wilson-Devinney code near the corresponding wavelength range; see Sect. 3.4. At the observed phases they range between about -1.2 and $+1.4$ $\mathrm{km\,s^{-1}}$ for the primary component and between about -2.2 and $+1.3$ $\mathrm{km\,s^{-1}}$ for the secondary component. Order to order differences are less than 10% of the corrections; using average corrections leads in fact to identical orbital solutions.

Next, for each observed phase, mean values of the corrected radial velocities from the eight selected orders were formed, and spectroscopic orbits were then calculated using the method of Lehman-Filhés implemented in the SBOP[4] program (Etzel 2004), which is a modified and expanded version of an earlier code by Wolfe, Horak & Storer (1967). A circular orbit was assumed, and the period P and epoch T were fixed at the ephemeris values (Eq. 1). Equal weights were assigned to the radial velocities, and the two components were analysed independently (SB1 solutions). The elements are listed in the first two columns of Table 7, and as seen, the results from the WD based and the simpler symmetrical BF's agree very well, giving minimum masses accurate to about 0.6%. For both set of velocities, SB2 analyses yield identical semiamplitudes. Within errors, the system velocities agree, even without accounting for the small difference in gravitational redshift for the components, about 0.06 $\mathrm{km\,s^{-1}}$.

As a further check, we have analysed the eight orders independently. The individual semiamplitudes differ slightly more than their typical mean errors of 0.6 $\mathrm{km\,s^{-1}}$, but for both BF methods, their mean values agree very well with the results presented in Table 7. Finally, applying instead mean radial velocities weighted according to the quality of the individual order solutions, and/or weighting the mean radial velocities according to the S/N ratio of the observed spectra (Table 5), lead to practically identical elements. Also, shifting first the velocities from each order by the difference between its system velocity and the mean system velocity (primary and secondary components treated individually) does not change the elements significantly.

Based on the results mentioned above, we believe that the radial velocity differences from the two BF approaches, which for the mean values are within ± 1 $\mathrm{km\,s^{-1}}$, are more likely due to imperfections in the observed BF's, affecting the theoretical fits differently, than to measurable (line) asymmetries. Furthermore, the quality of the two datasets are comparable with about the same order-to-order spread of the velocities. We have therefore taken the pragmatic decision to base the final orbital elements on the mean values of their velocities; see Table A.1. These elements are listed in the third column of Table 7 and the corresponding orbits are shown in Fig. 4. Finally, we note that if the light center velocities are applied without corrections, both semiamplitudes become 1.1 $\mathrm{km\,s^{-1}}$ smaller than listed in Table 7, and the derived masses become about 0.03 $M_\odot$ lower.

Our results differ slightly from those by Rucinski et al. (2003), $K_p = 160.11 \pm 0.74$ $\mathrm{km\,s^{-1}}$, $K_s = 147.21 \pm 0.63$ $\mathrm{km\,s^{-1}}$, and $\gamma = -12.74 \pm 0.46$ $\mathrm{km\,s^{-1}}$, and are more accurate.

[4] Spectroscopic Binary Orbit Program, http://mintaka.sdsu.edu/faculty/etzel/

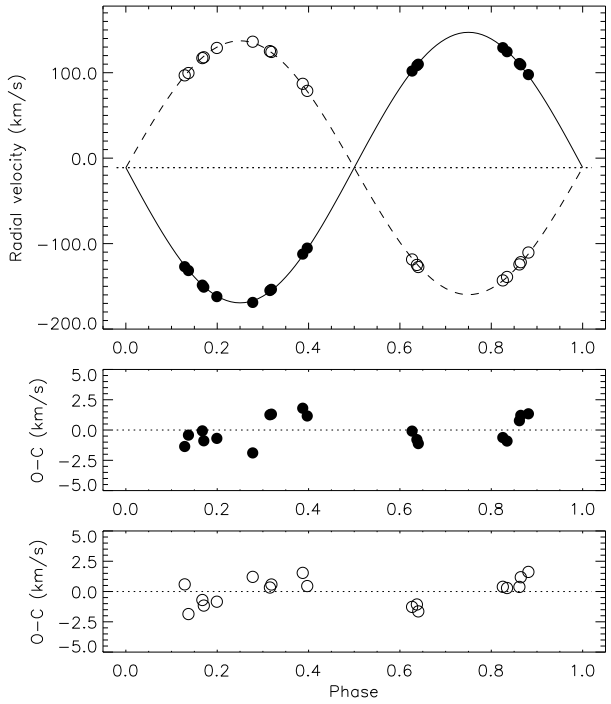

Fig. 4. Spectroscopic orbital solution for V1130 Tau (solid line: primary; dashed line: secondary) and corrected radial velocities (filled circles: primary; open circles: secondary). The dotted line (upper panel) represents the mean center-of-mass velocity of the system. Phase 0.0 corresponds to central primary eclipse.

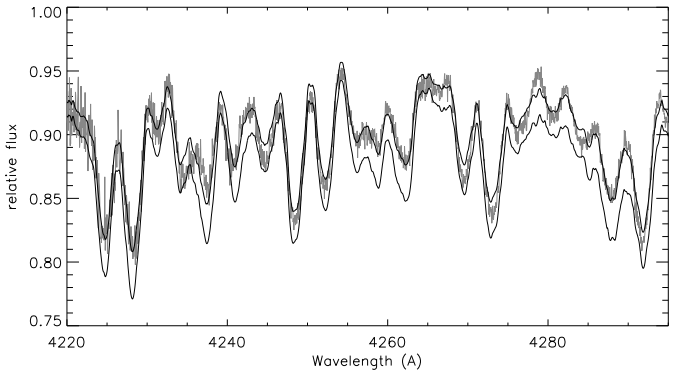

Fig. 5. Part of FEROS spectrum taken at phase 0.168 (gray) and synthetic binary spectra (thin) calculated for [Fe/H] = −0.25 (upper) and [Fe/H] = 0.00 (lower).

5. Chemical abundances

Due to the high rotational velocities of the components (Sect. 4.2), a detailed chemical analysis of V1130 Tau based on the FEROS spectra is difficult, see Fig. 5. First, the lines with intrinsic equivalent widths below about 100 mÅ, which should preferably be used, are shallow and broad and therefore impossible to measure accurately. Next, line blending becomes a serious issue, and finally proper normalization of the spectra is difficult, especially in the blue spectral region.

Table 8. Astrophysical data for V1130 Tau.

	Primary	Secondary
Absolute dimensions:		
$M/M_\odot$	1.306 ± 0.008	1.392 ± 0.008
$R/R_\odot$	1.489 ± 0.010	1.782 ± 0.011
$\log g$ (cgs)	4.208 ± 0.006	4.080 ± 0.006
$v \sin i$[a] ($\mathrm{km\,s^{-1}}$)	92.4 ± 1.1	104.7 ± 2.7
v_{sync}[b] ($\mathrm{km\,s^{-1}}$)	90.6 ± 0.6	108.5 ± 0.7
Photometric data:		
V	7.526 ± 0.014	7.128 ± 0.011
$(b-y)$	0.260 ± 0.004	0.265 ± 0.004
m_1	0.141 ± 0.008	0.140 ± 0.008
c_1	0.481 ± 0.010	0.476 ± 0.010
$E(b-y)$	0.000 ± 0.008	
$T_{\rm eff}$	6650 ± 70	6625 ± 70
$M_{\rm bol}$	3.27 ± 0.05	2.89 ± 0.05
$\log L/L_\odot$	0.59 ± 0.02	0.74 ± 0.02
BC	0.02	0.01
M_V	3.25 ± 0.05	2.88 ± 0.05
$V_0 - M_V$	4.28 ± 0.06	4.25 ± 0.06
Distance (pc)	71.6 ± 2.1	70.8 ± 2.1
Abundance:		
[Fe/H]	-0.25 ± 0.10	

[a] Observed rotational velocity
[b] *Projected* equatorial velocity for synchronous rotation

NOTE: Bolometric corrections (BC) by Flower (1996) have been assumed, together with $T_{eff\odot} = 5780$ K, $BC_\odot = -0.08$, and $M_{bol\odot} = 4.74$.

Line by line analyses of either the observed spectra or the reconstructed component spectra calculated from disentangled spectra have therefore not been attempted. We refer to CTB08 and Clausen et al. (2009) for details on line by line analyses of binaries. We have instead established upper and lower limits for the metal abundance of V1130 Tau by comparing the observed spectra and synthetic binary spectra calculated for a range of scaled solar compositions. The synthetic spectra were produced as described in Sect. 4.2. The overall result, based on inspection of several spectra and orders, is that synthetic spectra for metal abundances between -0.35 and -0.15 dex fit the observed spectra equally well, whereas e.g. the lines/lineblends for solar abundance spectra, as illustrated in Fig. 5, are clearly too strong.

In addition, abundances have been derived from various *uvby* calibrations and the indices listed in Tables 1 and 8. The Holmberg et al. (2007) calibration gives [Fe/H] = -0.25 ± 0.12 for both components, whereas the 'blue' calibration by Nordström et al. (2004) gives [Fe/H] = -0.34 ± 0.14. For comparison, the older calibration by Edvardsson et al. (1993) gives [Fe/H] = -0.27 ± 0.11.

In conclusion, we confirm that V1130 Tau is (slightly) metal-weak, see Sect. 2, and adopt [Fe/H] = -0.25 ± 0.10.

6. Absolute dimensions

Absolute dimensions for the components of V1130 Tau are calculated from the elements given in Tables 4 and 7. As seen in Table 8, both masses and (volume) radii have been established to an accuracy of 0.6–0.7%.

Individual standard *uvby* indices are included in Table 8, as calculated from the combined indices of V1130 Tau outside eclipses (Table 1) and the luminosity ratios (Table 4). According to the calibration by Olsen (1988) and the combined *uvbyβ* indices at phase 0.25, there is no significant interstellar reddening.

The adopted effective temperatures (6650 K, 6625 K) were calculated from the calibration by Holmberg et al. (2007), assuming [Fe/H] = −0.25 (Sect. 5). The uncertainties include those of the *uvby* indices, $E(b-y)$, [Fe/H] and the calibration itself. Identical temperatures are obtained from the calibration by Ramírez & Meléndez (2005), whereas that by Alonso et al. (1996) leads to 100 K lower values. 2MASS photometry at phase 0.79, where $V = 6.555$, and the $V - K_s$ calibration by Masana et al. (2006) gives an average temperature of 6600 K.

The measured rotational velocities ($v \sin i$) are close to the projected synchronous velocities. We note that for an orbital inclination of 'only' 73°.8, the true equatorial velocities are about 4% higher. The turbulent dissipation and radiative damping formalism of Zahn (1977, 1989) predicts synchronization times scales of 8.7×10^5 yr (primary) and 3.1×10^5 yr0.1 Gyr (secondary), and a time scale for circularization of 1.2×10^7 yr.

The distance to V1130 Tau was calculated from the 'classical' relation (see e.g. CTB08), adopting the solar values and bolometric corrections given in Table 8 and accounting for all error sources. Other *BC* scales (e.g. Code et al. 1976, Bessell et al. 1998, Girardi et al. 2002) give nearly identical results. As seen, the distances obtained for the two components agree well. The mean distance, 71.2 pc, which has been established to about 3%, is close to the result from the new Hipparcos reduction by van Leeuwen (2007), 69.8 ± 2.3 pc, but is marginally larger than the original Hipparcos result 65.2 ± 3.3 pc (ESA 1997). Finally, we note that V1130 Tau belongs to the group of eclipsing binaries within 125 pc, discussed by Popper (1998), which could be useful for improving the radiative flux scale.

7. Discussion

Below, we first compare the absolute dimensions obtained for V1130 Tau with properties of recent theoretical stellar evolutionary models, and we then discuss V1130 Tau together with the few other similar well-studied eclipsing binaries available.

7.1. Comparison with stellar models

Figs. 6, 7, and 8 illustrate the results from comparisons with the Yonsei-Yale (Y^2) evolutionary tracks and isochrones by Demarque et al. (2004)[5]. They include core overshoot where $\Lambda_{OS} = \lambda_{ov}/H_p$ depends on mass and also takes into account the composition dependence of M^{conv}_{crit} [6]. The mixing length parameter in convective envelopes is calibrated using the Sun, and is held fixed at $l/H_p = 1.7432$. The enrichment law $Y = 0.23 + 2Z$ is adopted, together with the solar mixture by Grevesse et al. (1996), leading to $(X,Y,Z)_\odot$ = (0.71564,0.26624,0.01812). A brief description of other aspects of their up-to-date input physics in given by CTB08. Only models for [α/Fe] = 0.0 have been included in the figures. We have used the abundance, mass, and age interpolation routines provided by the Y^2 group.

As seen from Fig. 6, models for the observed masses and abundance, [Fe/H] = −0.25, equivalent to $(X,Y,Z)_\odot$

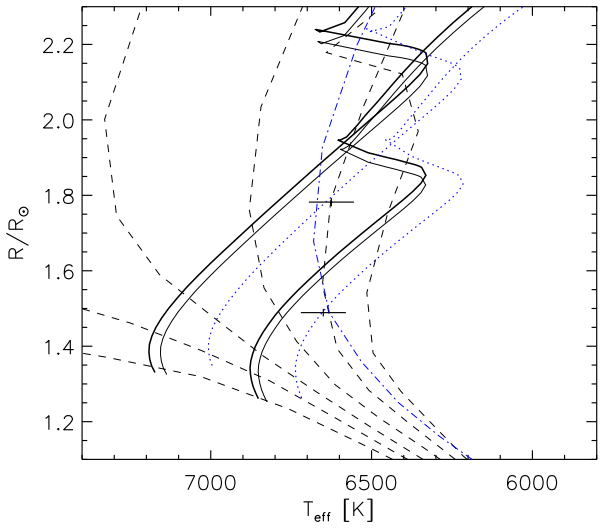

Fig. 6. V1130 Tau compared to Y^2 models calculated for [Fe/H] = −0.25. Tracks for the component masses (full drawn, thick) and isochrones for 0.5–3.0 Gyr (dashed, step 0.5 Gyr) are shown. The uncertainty in the location of the tracks coming from the mass errors are indicated (full drawn, thin). To illustrate the effect of the abundance uncertainty, tracks (dotted, blue) and the 2.2 Gyr isochrone (dash-dot, blue) for [Fe/H] = −0.15 are included.

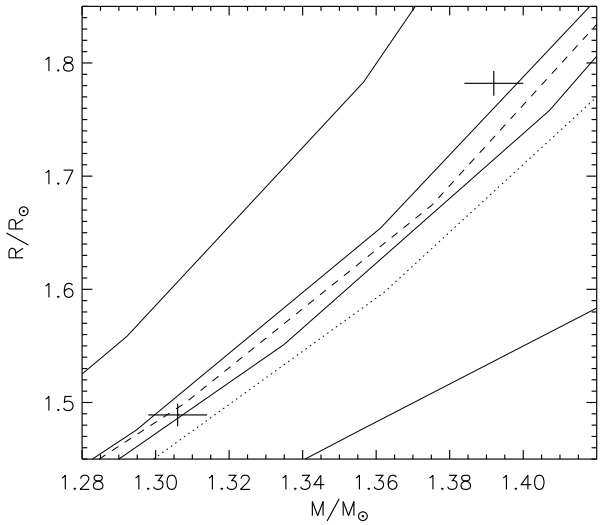

Fig. 7. V1130 Tau compared to Y^2 models calculated for [Fe/H] = −0.25. Isochrones (full drawn) for 1.5, 2.0, 2.13, and 2.5 Gyr are shown. To illustrate the effect of the abundance uncertainty, 2.0 Gyr isochrones for [Fe/H] = −0.15 (dotted) and [Fe/H] = −0.35 (dashed) are included.

[5] http://www.astro.yale.edu/demarque/yystar.html

[6] Defined as "the mass above which stars continue to have a substantial convective core even after the end of the pre-MS phase."

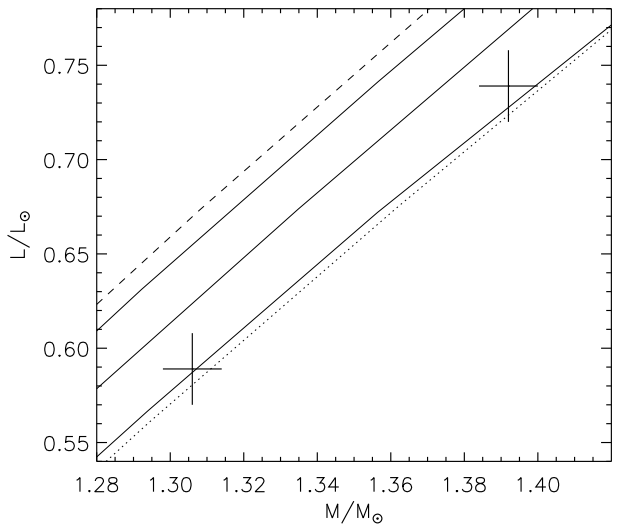

Fig. 8. V1130 Tau compared to Y^2 models calculated for [Fe/H] = −0.25. Isochrones (full drawn) for 1.5, 2.0, and 2.5 Gyr are shown. To illustrate the effect of the abundance uncertainty, 2.0 Gyr isochrones for [Fe/H] = −0.15 (dotted) and [Fe/H] = −0.35 (dashed) are included.

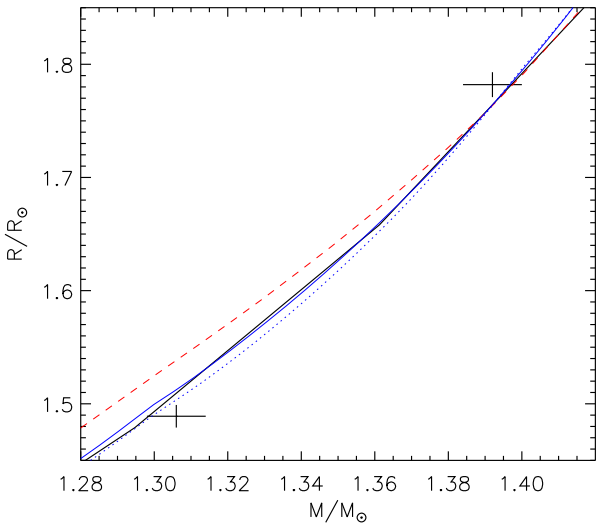

Fig. 9. V1130 Tau compared to the models listed in Table 9. Isochrones for the average ages inferred from masses and radii are shown. Y^2: thick full drawn (black). BaSTI overshoot: thin full drawn (blue). BaSTI standard: dotted (blue). Victoria-Regina: dashed (red).

= (0.7385,0.2510,0.0105), are about 200 K hotter than observed. The uncertainty of [Fe/H] is ±0.10 dex, and tracks for [Fe/H] = −0.15, equivalent to (X,Y,Z) = (0.7310,0.2560,0.0130), fit the components at an age of about 2.2 Gyr. This can also be reached for [Fe/H] = −0.25, if a slight hypothetical α-element enrichment of [α/Fe] = 0.15 is introduced. The more massive secondary component has evolved to the middle of the main sequence band.

From a binary perspective, the most fundamental comparison is that based on the scale-independent masses and radii, as shown in Fig. 7. The [Fe/H] = −0.25 model isochrone for 2.13 Gyr marginally fits both components, but within the abundance uncertainty, the general trend is that the Y^2 isochrones predict a higher age for the secondary component than for the primary. Although less evident, this is also seen in the mass–luminosity diagram (Fig. 8).

Table 9. Models information and average ages inferred from masses and radii; see Fig. 9.

Grid	[Fe/H]	Y	Z	Age (Gyr)
Yonsai-Yale (Y^2)	−0.25	0.2510	0.0105	2.13
Victoria-Regina	−0.29	0.2574	0.0100	1.98
BaSTI (overshoot)	−0.25	0.2590	0.0100	1.84
BaSTI (standard)	−0.25	0.2590	0.0100	1.80

In Fig. 9 we have included mass-radius comparisons with the Victoria-Regina (VRSS grid; VandenBerg et al., 2006)[7] and BaSTI (Pietrinferni et al., 2004)[8] models, which differ from Y^2, e.g. with respect to input physics, He enrichment law, and core overshoot treatment. We refer to CTB08 for a brief description. Basic parameters for the models, all with solar scaled abundances, are given in Table 9. Like the Y^2 models, both the standard and overshoot BaSTI models marginally fit both components, but at a lower age. However, the Victoria-Regina models do not fit V1130 Tau well. To us, this is surprising, because these models are carefully calibrated by cluster and binary observations. Models with [α/Fe] = 0.3 (VR2A grid) can reproduce V1130 Tau at an age of about 2.15 Gyr, but only for [Fe/H] around -0.40 dex.

Thus, except for the Victoria-Regina models, all the models with solar scaled abundances we have tested are marginally able to reproduce V1130 Tau, but we see two general trends: First, models for the observed [Fe/H] are about 200 K too hot. Second, they systematically predict higher ages for the more massive secondary component than for the primary. In order to look in more detail into this, we have calculated dedicated models for the component masses with various parameters tuned. For all models, we have adopted Z = 0.010, which is equivalent to the observed [Fe/H]. We have applied the Granada code by Claret (2004), which assumes an enrichment law of $Y = 0.24+2.0Z$ together with the solar mixture by Grevesse & Sauval (1998), leading to $(X,Y,Z)_\odot$ = (0.704,0.279,0.017). The envelope mixing length parameter needed to reproduce the Sun is l/H_p = 1.68. The amount of core overshooting is given, in units of the pressure scale height, by α_{ov}.

Table 10 lists the models we have investigated. As seen in Fig. 10, the overshoot models (1) with Y calculated from the adopted enrichment law are too hot, as seen for the other grids. The same is true for models without overshoot (2, not shown). Since the components of V1130 Tau are rotating quite fast (Table 8), we have calculated models which include rotation as described by Claret (1999). Angular velocities for the models were tuned to reproduce the observed equatorial rotational velocities of the components. As expected, such models (3) are cooler than similar ones without rotation (1), but the effect is small compared to the about 200 K discrepancy. Next, the components of

[7] http://www1.cadc-ccda.hia-iha.nrc-cnrc.gc.ca/cvo/community/VictoriaReginaModels/

[8] http://www.te.astro.it/BASTI/index.php

Table 10. Information on the Claret models and ages inferred from radii; see Figs. 10 and 11.

Model/ Linestyle	Y	Z	l/H_p	α_{ov}	Rotation	Age (Gyr) Primary	Age (Gyr) Secondary
1 thin, blue	0.260	0.010	1.68	0.20	NO	2.08 ± 0.07	2.24 ± 0.03
2	0.260	0.010	1.68	0.00	NO	2.01 ± 0.07	2.14 ± 0.03
3 dotted, blue	0.260	0.010	1.68	0.20	YES	2.01 ± 0.07	2.19 ± 0.03
4 dashed, blue	0.260	0.010	1.50	0.20	NO	1.98 ± 0.07	2.20 ± 0.03
5 thick, black	0.240	0.010	1.68	0.20	NO	2.51 ± 0.07	2.60 ± 0.04
6	0.230	0.010	1.68	0.20	NO	2.75 ± 0.07	2.81 ± 0.04

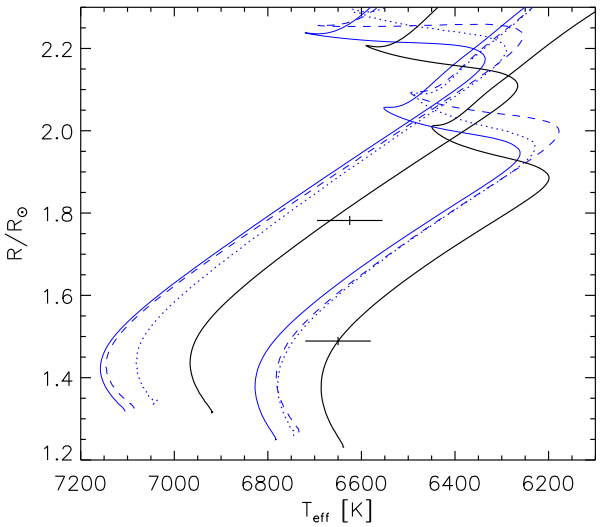

Fig. 10. V1130 Tau compared to Claret models for the observed masses and [Fe/H] abundance. See Table 10 for details and linestyles/colours.

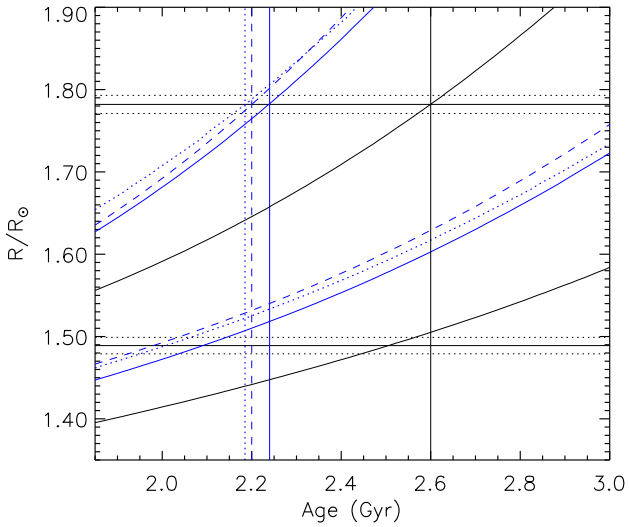

Fig. 11. V1130 Tau compared to Claret models for the observed masses and [Fe/H] abundance. See Table 10 for details. The curves illustrate model radii as function of age for the components (upper: secondary; lower: primary). The horizontal full drawn lines mark the observed radii of the components with errors (dotted lines). The vertical lines mark the ages predicted for the secondary component.

V1130 Tau have (thin) outer convection zones, and we have therefore investigated the effect of modifying the envelope mixing length parameter. 2D radiation hydrodynamic calculations by Ludwig et al. (1999; see also Clausen et al. 2009) predict parameters, which are about 0.2 lower than for the Sun, and we have therefore adopted 1.50. The models (4) become cooler, but again the effect is too small. Finally, we have calculated models with a He abundance slightly lower than $Y = 0.26$, as given by the enrichment law for $Z = 0.01$. Tracks for $Y = 0.24$ (5) and 0.23 (6, not shown) actually fit V1130 Tau well. If we now turn to the ages, as determined from the radii, Fig. 11 shows that these models with lower Y also predict practically identical ages for the components. In fact, this also holds if lower α_{ov} values are adopted; models without overshoot place the primary component just at the end of the core hydrogen burning phase. On the other hand, all the Granada models for $Y = 0.26$ predict higher ages for the secondary component than for the primary, as seen for the other grids.

Before finishing these comparisons and drawing any definite conclusions about the need to adjust basic physical or chemical ingredients of the models, it is worth remembering that besides being fast rotating, the components of V1130 Tau are influenced by their mutual gravitational and radiative interactions. They cause not only additional deformation, but also expansion and some heating, and these effects are probably somewhat different for the two stars. We will not elaborate further on the possible implications for the model comparisons until additional, similar, but more detached binaries have been studied.

7.2. Comparison with other binaries

Binaries like V1130 Tau with component(s) that have evolved to the upper half of the main sequence band, or beyond, may give important information on core overshoot. Already 20 years ago, such systems were found to provide strong evidence for convective core overshoot in intermediate mass (1.5–2.5 $M_\odot$) stars (Andersen et al. 1990). From a sample of 2–12 $M_\odot$ systems, Ribas et al. (2000) found a significantly increasing of the amount of overshoot with increasing stellar mass, whereas Claret (2007) found that it is less pronounced and more uncertain.

From the onset of core convection up to about 1.5 $M_\odot$ there are, however, only a few relevant, well-studied binaries: (excluding active systems and systems with nearly identical components): AI Phe, BK Peg, BW Aqr, and GX Gem. Andersen et al. (1988) found that models without core overshoot were able to reproduce AI Phe (1.24 + 1.20 $M_\odot$, components above the main sequence) remarkably

well for a normal helium abundance[9], whereas Clausen (1991) found that models including moderate overshoot gave better fits for especially the primary components of the slightly more massive systems BW Aqr (1.49 + 1.39 $M_\odot$) and BK Peg (1.43 + 1.28 $M_\odot$). The latter is consistent with a lower limit of α_{ov} of about 0.18 for GX Gem (1.49 + 1.47 $M_\odot$), as established by Lacy et al. (2008).

We had hoped and expected, that V1130 Tau could fill the mass gap between these systems, but as mentioned in Sect. 7.1 this is not the case - Claret models with α_{ov} from 0 to at least 0.2 can reproduce it perfectly well for Y = 0.23–0.24. In contradiction to this, Tomasella et al. (2008a, 2008b) report determination of α_{ov} from the much younger systems V505 Per and V570 Per.

It is, however, still important to try to calibrate core overshoot better from its onset to say 2 $M_\odot$. For the Victoria-Regina model grids, VandenBerg et al. (2006) adopt, from binary and cluster information, a mass and abundance dependent amount, setting in around 1.1 $M_\odot$ and gradually increasing up to about 1.7 $M_\odot$. Demarque et al. (2004) apply a different ramping algorithm for the Y^2 isochrones, as do Pietrinferni et al. (2004) for the BaSTI calculations. These recipes, and others, need further empirical tests, and we plan to address that issue in forthcoming re-analyses of BW Aqr and BK Peg, which will include abundance determinations, as well as through new complete analyses of AL Leo, HD76196, and possibly also the NGC752 member DS And.

Another important aspect is the He abundance and the helium-to-metal enrichment ratio, and, through extrapolation, the primordial He/H abundance ratio. As discussed in Sect. 7.1, V1130 Tau points towards a lower He abundance and/or enrichment ratio than the four different Y, Z prescriptions adopted by the model grids studied. We refer to Casagrande et al. (2007) for at recent determination of $\Delta Y/\Delta Z$ based on K dwarfs (2.1±0.9), to Blaser (2006) for a HII based study (1.41 ± 0.62) with references to a variety of methods and results, and to Ribas et al. (2000) and Claret & Willems (2002) for determinations based on samples of eclipsing binaries (2.2 ± 0.8 and 1.9 ± 0.6, respectively). We believe binaries can give an even better constraint, provided detailed heavy element abundance determinations become available for a sufficiently large sample[10]. Such investigations are in progress for several systems, and we will return to this matter in forthcoming papers.

Here, we close the issue with a brief historical remark: The use of binaries to determine the hydrogen content of stars was pioneered by Eddington (1932) and Strömgren (1932, 1933), and a few years later Strömgren (1938) also used binaries in his classical discussion of the helium content of the interior of the stars. Later, binary based helium-hydrogen abundance ratio determinations (for Population I stars) were published by Strömgren (1967) and Popper et al. (1970).

8. Summary and conclusions

From state-of-the-art observations and analyses, precise (0.6–0.7%) absolute dimensions have been established for the nearby, early F-type, double-lined, detached eclipsing binary V1130 Tau. From synthetic spectra and *uvby* calibrations, a metal abundance of [Fe/H] = -0.25 ± 0.10 has been derived. The 1.39 $M_\odot$ secondary component has evolved to the middle of the main-sequence band and is slightly cooler than the 1.31 $M_\odot$ primary. The $P = 0\overset{\mathrm{d}}{.}80$ period orbit is circular and the observed rotational velocities of the components, 92.4 ± 1.1 (primary) and 104.7 ± 2.7 (secondary) km s^{-1}, correspond closely to synchronization.

Yonsai-Yale, BaSTI, and Granada evolutionary models for the observed metal abundance and a 'normal' He content of $Y = 0.25 - 0.26$, as established from the adopted helium enrichment laws, marginally reproduce the components at ages between 1.8 and 2.1 Gyr. All such models are, however, systematically about 200 K hotter than observed, and predict ages for the more massive component, which are systematically higher than for the less massive component. The latter is even more pronounced for Victoria-Regina models. The two trends can not be removed by adjusting the amount of core overshoot or envelope convection level, or by including rotation in the model calculations. They may be due to proximity effects in V1130 Tau, but on the other hand, we find excellent agreement for 2.5–2.8 Gyr Granada models with a slightly lower Y of 0.23–0.24.

We had expected that V1130 Tau is sufficiently evolved to provide new information on the level of core overshoot in the 1.1–1.7 $M_\odot$interval, where it is believed to ramp up, but this is not the case. V1130 Tau can be reproduced by models calculated for α_{ov} from 0.0 to at least 0.2. The preference for a helium content of 0.23–0.24 is interesting, but more well-detached systems with measured metal abundances are needed for any firm conclusions on the implications for example for the helium enrichment law. We will return to these issues in forthcoming papers on other systems recently observed within the Copenhagen binary project.

Acknowledgements. We thank B. R. Jørgensen, J. Mouette, and N. T. Kaltcheva for participating in the (semi)automatic observations of V1130 Tau at the SAT. A. Kaufer, O. Stahl, S. Tubbesing, and B. Wolf kindly obtained seven FEROS spectra of V1130 Tau during Heidelberg/Copenhagen guaranteed time in 1999. Excellent technical support was received from the staffs of Copenhagen University and ESO, La Silla. We thank J. M. Kreiner for providing a complete list of published times of eclipse for V1130 Tau, H. Bruntt for making his *bssynth* software available, and J. Southworth for access to his JKTWD code.

The projects "Stellar structure and evolution – new challenges from ground and space observations" and "Stars: Central engines of the evolution of the Universe", carried out at Copenhagen University and Aarhus University, are supported by the Danish National Science Research Council.

The following internet-based resources were used in research for this paper: the NASA Astrophysics Data System; the SIMBAD database and the VizieR service operated by CDS, Strasbourg, France; the arχiv scientific paper preprint service operated by Cornell University; the VALD database made available through the Institute of Astronomy, Vienna, Austria. This publication makes use of data products from the Two Micron All Sky Survey, which is a joint project of the University of Massachusetts and the Infrared Processing and Analysis Center/ California Institute of Technology, funded by the National Aeronautics and Space Administration and the National Science Foundation.

[9] see also Torres et al. 2009

[10] see Torres et al. (2009) Table 3 for the limited material available today

References

Abt, H. A. 1986, ApJ, 309, 260
Alonso, A., Arribas, S., & Martínez-Roger, C. 1996, A&A, 313, 873
Andersen, J., Clausen, J. V., Gustafsson, B., Nordström, B., & VandenBerg, D. A. 1988, A&A, 196, 128
Andersen, J., Nordström, B., & Clausen, J. V. 1990, ApJ, 363, L33
Balser, D. S. 2006, AJ, 132, 2326

Bessell, M. S., Castelli, F., & Plez, B. 1998, A&A, 333, 231
Brat, L., Smelcer, L., Kucakova, H. et al. 2008, Open Eur. Jour. Var. Stars, 94, 1
Casagrande, L., Flynn, C., Portinari, L., Girardi, L., & Jimenez, R. 2007, MNRAS, 382, 1516
Claret, A., 1999, A&A, 350, 56
Claret, A., 2000, A&A, 363, 1081
Claret, A., 2004, A& A,424, 919
Claret, A. 2007, A&A, 475, 1019
Claret, A. & Willems, B. 2002, A&A, 388, 518
Clausen, J. V. 1991, A&A, 246, 397
Clausen, J. V., Helt, B. E., & Olsen, E. H. 2001, A&A, 374, 980 (CHO01)
Clausen, J. V., Torres, G., Bruntt, H., et al. 2008, A&A, 487, 1095 (CTB08)
Clausen, J. V., Bruntt, H., Claret, A. et al. 2009, A&A, 502, 353
Code, A. D., Bless, R. C., Davis, J., & Brown, R. H. 1976, ApJ, 203, 417
Demarque, P., Woo, J.-H., Kim, Y.-C., & Yi, S. K. 2004, ApJS, 155, 667
Eddington, A. S., MNRAS, 92, 471
Edvardsson, B., Andersen, J., Gustafsson, B. et al. 1993, A&A, 275, 101
ESA 1997, The Hipparcos and Tycho Catalogues, ESA SP-1200
Etzel, P. B. 2004, SBOP: Spectroscopic Binary Orbit Program San Diego State University)
Flower, P. J. 1996, ApJ, 469, 355
Franco, G. A. P. 1988, A&AS, 74, 73
Grevesse, N, & Sauval, A. J. 1998, Space Sci. Rev., 85, 161
Grevesse, N., Noels, A., & Sauval, A. J. 1996, in Cosmic Abundances, eds. S.S. Holt & G. Sonneborn (San Francisco: ASP), 117
Girardi, L., Bertelli, G., Bressan, A., et al. 2002, A&A, 391, 195
Gray, R. O. 1989, AJ, 98, 1049
Gray, R. O., & Garrison, R. F. 1989, ApJS, 69, 301
Gray, R. O., Napier, M. G., & Winkler, L. I. 2001, AJ, 121, 2148
Heiter, U., Kupka, F., van't Menneret, C. et al. 2002, A&A, 392, 619
Holmberg, J., Nordström, B., & Andersen, J. 2007 A&A, 475, 519
Houk, N. & Swift, C. 1999, Michigan Catalogue of two-dimensional spectraltypes for HD stars. Vol. 5, Dep. Astron., Univ. Michigan, Ann Arbor, Michigan, USA
Kaluzny, J., Pych, W., Rucinski, S. M., & Thompson, I. B. 2006, Acta Astron., 56, 237
Kaufer, A., Stahl, O., Tubbesing, S., et al. 1999, The ESO Messenger, 95, 8
Kaufer, A., Stahl, O., Tubbesing, S., et al. 2000, in Proc. SPIE 4008, Optical and IR Telescope Instrumentation and Detectors, ed. M. Iye & A. F. Morwood, 459
Kazarovets, E. V., Samus, N. N., Durlevich, O.V. et al. 1991, Inf. Bull. Var. Stars, 4659
Kreiner, J. M., Kim, C. H., & Nha, I. S. 2001, An Atlas of O−C Diagrams of Eclipsing Binary Stars (Krakow: Wydawnictwo Naukowe Akad. Pedagogicznej)
Kreiner, J: M. 2004, Acta Astron., 54, 207
Kupka, F., Piskunov, N., Ryabchikova, T. A., Stempels, H. C., & Weiss, W. 1999, A&AS, 138, 119
Kurucz, R. L., 1993, in Light Curve Modelling of Eclipsing Binary Stars, ed., E. F. Milone, Springer Verlag, 93
Lacy, C. H. S., Torres, G., & Claret, A. 2008, AJ, 135, 1757
Ludwig, H:-G., Freytag, B, & Steffen, M. 1999,
Masana, E., Jordi, C., & Ribas, I. 2006, A&A, 450, 735
Nordström, B., Mayor, M., Andersen, J., et al. 2004, A&A, 418, 989
Olsen, E.H. 1983, A&AS, 54, 55
Olsen, E. H. 1988, A&A, 189, 173
Olsen, E.H. 1993, A&AS, 102, 89
Olsen, E. H. 1994, A&AS, 106, 257
Pavlovski, K., Tamajo, E., Koubský, P., et al. 2009, astro-ph/09080351
Pietrinferni, A., Cassisi, S., & Salaris, M. 2004, Mem. Soc. Astron. Italiana, 75, 170
Popper, D. M. 1983, AJ, 88, 124
Popper, D. M. 1998, PASP, 110, 919
Popper, D. M., Jœrgensen, H. E., Morton, D. C., & Leckrone, D. S. 1970, ApJ, 161, L57
Ramírez, I., & Meléndez, J. 2005, AJ, 626, 465
Ribas, I., Jordi, C., & Giménez, A. 2000, MNRAS, 318, L55
Ribas, I., Jordi, C., Torra, J., & Giménez, A. 2000, MNRAS, 313, 99
Rucinski, S. M. 1999, in Hearnshaw, J. B. & Scarfe, C. D. (eds) IAU Coll. 170 Precise Stellar Radial Velocities, ASP Conference Series 185, 82
Rucinski, S. M. 2002, AJ, 124, 1746
Rucinski, S. M. 2004, in Maeder, A. & Eenens, P. (eds) IAU Symp. 215 Stellar Rotation, ASP Conference Series, p.17
Rucinski, S. M., Lu, W. X., & Shi, J. 1993, AJ106, 1174
Rucinski, S. M., Capobianco, S. C., Lu, W., et al. 2003, AJ, 125, 3257
Southworth, J., & Clausen, J. V. 2007, A&A, 461, 1077
Strömgren, B. 1932, ZAp, 4, 118
Strömgren, B. 1933, ZAp, 7, 222
Strömgren, B. 1938, ApJ, 87, 520
Strömgren, B. 1967, in Modern Astrophysics: A Memorial to Otto Struve, ed. M. Hack, 185
Tomasella, L., Munari, U., Siviero, A. et al. 2008a, A&A, 480, 465
Tomasella, L., Munari, U., Cassisi, S. et al. 2008b, A&A, 483, 263
Torres, G., Andersen, J., & Giménez, A. 2009, A&A Rev., in press
Valenti, J., & Piskunov, N. 1996, A&AS, 118, 595
VandenBerg, D. A., Bergbusch, P. A., & Dowler, P. D. 2006
Van Hamme, W., 1993, AJ, 106, 2096
Van Hamme, W., & Wilson, R. E. 2003, in ASP Conf. Ser. 298, GAIA Spectroscopy: Science and Technology, ed. U. Munari (San Fransisco: ASP), 323
van Leeuwen, F. 2007, Hipparcos, the new reduction of the raw data (Dordrecht: Springer)
Wilson, R. E. 1979, ApJ, 234, 1054
Wilson, R. E. 1990, ApJ, 356, 613
Wilson, R. E. 1993, in ASP Conf. Ser. 38, New Frontiers in Binary Star Research, ed. K. C. Leung & I. S. Nha (San Fransisco: ASP), 91
Wilson, R. E., & Devinney, E. J. 1971, ApJ, 166, 605
Wolfe, R. H., Horak, H. G., Storer, N. W., 1967, in Modern Astrophysics: A Memorial to Otto Struve, ed. M. Hack, 251
Zahn, J.-P. 1977, A&A, 57, 383
Zahn, J.-P. 1989, A&A, 220, 112

List of Objects

Appendix A: Radial velocity observations

List of Objects

Table A.1. Mean radial velocities for V1130 Tau.

HJD − 2 400 000	Phase	RV_p [a]	δRV_p [b]	$O-C$ [c]	RV_s [a]	δRV_s [b]	$O-C$ [c]
51188.63785	0.16750	−147.46	1.16	−0.07	115.92	−1.16	−0.70
51207.54462	0.83445	123.44	−1.14	−0.91	−137.91	1.12	0.29
51207.56623	0.86150	109.88	−0.86	0.77	−123.77	0.60	0.38
51208.58523	0.13705	−130.70	0.84	−0.42	99.00	−0.58	−1.86
51209.59181	0.39706	−105.16	0.12	1.16	79.91	1.18	0.45
51211.56298	0.86451	108.40	−0.83	1.21	−121.21	0.55	1.18
51212.60641	0.17065	−149.78	1.18	−0.89	116.82	−1.23	−1.16
51385.92739	0.12883	−126.25	0.75	−1.36	96.42	−0.45	0.59
51386.93266	0.38720	−112.11	0.18	1.80	87.83	0.84	1.54
51390.86963	0.31539	−154.09	0.83	1.26	123.86	−1.39	0.33
51391.91712	0.62660	101.65	−0.27	−0.09	−119.05	−0.49	−1.27
51392.87464	0.82520	128.06	−1.22	−0.62	−141.76	1.32	0.39
51562.53347	0.19921	−160.66	1.39	−0.69	127.13	−1.82	−0.84
51562.59618	0.27771	−167.63	1.21	−1.89	134.03	−2.23	1.21
51562.62891	0.31868	−152.73	0.79	1.31	122.97	−1.29	0.58
51977.49585	0.63709	107.92	−0.35	−0.79	−125.16	−0.17	−1.07
51978.48974	0.88122	97.12	−0.65	1.34	−110.12	0.31	1.62
51981.49266	0.64018	109.54	−0.38	−1.12	−127.48	−0.07	−1.64

[a] Mean values of the *measured* radial velocities ($\mathrm{km\,s^{-1}}$)

[b] Mean correstions. Approximate center of mass velocities are obtained by subtracting these corrections ($\mathrm{km\,s^{-1}}$) from the measured velocities. For the orbital solutions, individual corrections were used for each order.

[c] $O-C$ residuals ($\mathrm{km\,s^{-1}}$) from the adopted spectroscopic orbits (Table 7).